Available online at www.sciencedirect.com
SCIENCE DIRECT
Journal of Solid State Chemistry 179 (2006) 1821–1829
JOURNAL OF SOLID STATE CHEMISTRY
www.elsevier.com/locate/jssc

Synthesis of nanocrystals in $KNb(Ge,Si)O_5$ glasses and chemical etching of nanocrystallized glass fibers

Itaru Enomoto, Yasuhiko Benino, Takumi Fujiwara, Takayuki Komatsu*

Department of Materials Science and Technology, Nagaoka University of Technology, 1603-1 Kamitomioka-cho, Nagaoka 940-2188, Japan

Received 11 January 2006; received in revised form 5 March 2006; accepted 10 March 2006
Available online 27 March 2006

Abstract

The nanocrystallization behavior of $25K_2O-25Nb_2O_5-(50-x)GeO_2-xSiO_2$ glasses with $x = 0, 25,$ and50 (i.e., $KNb(Ge,Si)O_5$ glasses) and the chemical etching behavior of transparent nanocrystallized glass fibers have been examined. All glasses show nanocrystallization, and the degree of transparency of the glasses studied depends on the heat treatment temperature. Transparent nanocrystallized glasses can be obtained if the glasses are heat treated at the first crystallization peak temperature. Transparent nanocrystallized glass fibers with a diameter of about 100 μm in $25K_2O–25Nb_2O_5–50GeO_2$ are fabricated, and fibers with sharpened tips (e.g., the taper length is about 450 μm and the tip angle is about 12°) are obtained using a meniscus chemical etching method, in which etching solutions of 10 wt%-HF/hexane and 10 M-NaOH/hexane are used. Although the tip (aperture size) has not a nanoscaled size, the present study suggests that $KNb(Ge,Si)O_5$ nanocrystallized glass fibers have a potential for new near-field optical fiber probes with high refractive indices of around $n = 1.8$ and high dielectric constants of around $\varepsilon = 58$ (1 kHz, room temperature).

Keywords: Nanocrystallization; Raman scattering spectra; Glass fiber; Chemical etching; Fiber probes

1. Introduction

Nanostructures are the gateway into a realm in physical, chemical, biological and materials science. Developing techniques for fabricating nanostructures inexpensively is an area that requires substantial effort. Crystallization of glass is one of the effective methods for fabrication of nanostructures [1]. Recently, transparent nanocrystallized glasses consisting of nonlinear optical/ferroelectric nanocrystals have received much attention, because such materials have a high potential for applications in photonic devices [2–6]. For instance, TeO_2-based nanocrystallized glasses showing a second harmonic generation (SHG) have been successfully fabricated [2–4].

Very recently, it has been found that a glass with the composition of $25K_2O–25Nb_2O_5–50GeO_2$ (i.e., $KNbGeO_5$) shows a prominent nanocrystallization [7–9]. Although second-order optical nonlinearities have not been detected from transparent nanocrystallized $KNbGeO_5$ glasses, elastic and mechanical properties of $KNbGeO_5$ glass have largely improved through nanocrystallization [7,8]. The crystallization behavior of the glass system of $K_2O–Nb_2O_5–SiO_2$ has been also studied, and the crystallized glasses showing SHGs have been fabricated [10–15]. In particular, the possibility of the formation of nanocrystals showing SHGs in $K_2O–Nb_2O_5–SiO_2$ glasses has been proposed [12,13,15]. Considering the features in crystallization and optical properties of $K_2O–Nb_2O_5–GeO_2$ and $K_2O–Nb_2O_5–SiO_2$ glass systems, it is of interest to study the crystallization behavior of $K_2O–Nb_2O_5–GeO_2–SiO_2$ glasses, and information might lead to the fabrication of transparent nanocrystallized glasses showing SHGs in this glass system.

On the other hand, as practical applications of transparent nanocrystallized glasses, the fabrication of nanocrystallized glass fibers is of interest [16–18]. Furthermore, among nanoscale science and technology, scanning near-field optical microscope (SNOM) absorbs great interests, in which usually optical glass fiber probes with sharpened tips have been used [19–21]. At this moment, however, it is unclear whether commercially available SiO_2-based glass

*Corresponding author. Fax: +81 258 47 9300.
E-mail address: komatsu@chem.nagaokaut.ac.jp (T. Komatsu).

0022-4596/$ - see front matter © 2006 Elsevier Inc. All rights reserved.
doi:10.1016/j.jssc.2006.03.028

fibers are best for near-field optical fiber probes or not. Considering the physical concept for the generation of near-field light at around the surface of particle, nanoparticles or sharpened tip fibers consisting of materials with high refractive indices (high dielectric constants) are favorable for near-field optical probes. In such materials, the generation of high intense near-field light would be expected through the generation of electric dipoles under light irradiation [22]. The refractive index (n) of SiO_2 glass is $n = 1.45$, as well-known. On the other hand, transparent nanocrystallized $KNbGeO_5$ glasses have the value of around $n = 1.8$ [7–9]. In this point of view, it is of particular interest to fabricate optical fiber probes consisting of nanocrystals with high refractive indices, i.e., nanocrystallized glass fiber probes. There has been no report on nanocrystallized glass fiber probes and also chemical etching of glass fibers consisting of nanocrystals so far.

In this study, we focus our attention on the nanocrystallization of $25K_2O$–$25Nb_2O_5$–$(50-x)GeO_2$–$xSiO_2$ glasses (i.e., $KNb(Ge,Si)O_5$ glasses) and the chemical etching of transparent nanocrystallized glass fibers. We clarified the formation behavior of nanocrystals in KNb(Ge,Si) glasses and optical properties of nanocrystallized glasses. Furthermore, we found a possibility for the fabrication of nanocrystallized glass fiber probes with sharpened tips by using a chemical etching technique.

2. Experimental

Glass compositions examined in the present study are shown in Table 1. Commercial powders of reagent grade K_2CO_3, Nb_2O_5, GeO_2 and SiO_2 were mixed and melted in a platinum crucible at 1200–1450 °C for 1 h in an electric furnace. The melts were poured onto an iron plate and pressed to a thickness of about 1 mm with another iron plate. The glass transition, T_g and crystallization peak, T_p temperatures were determined using differential thermal analyzes (DTA) at a heating rate of 10 K/min. Densities of glasses, d, were determined with the Archimedes method using distilled water as an immersion liquid. Refractive indices at a wavelength of 632.8 nm (He–Ne laser), n, were measured at room temperature with an ellipsometer (Mizojiri Opticals, DVA-36 model).

Glasses were heat treated at various temperatures for 3 h and crystalline phases present in the heat-treated samples were examined by X-ray diffraction (XRD) analyzes at room temperature using Cu$K\alpha$ radiation for powder (pulverized) samples. Optical transmission spectra were taken in the wavelength range of 190–2500 nm on a Shimazu UV-3150 spectrometer. Micro-Raman scattering spectra at room temperature for the precursor glasses and crystallized samples were measured with a laser microscope (Tokyo Instruments Co., Nanofinder) operated at Ar^+ (488 nm) laser. In our micro-Raman apparatus, the data below $\sim 300\,cm^{-1}$ cannot be measured due to the use of edge filter. SHGs of crystallized powders at room temperature were examined using the powder method proposed by Kurtz and Perry [23]. A fundamental wave of a Q-switched Nd:YAG laser operating at a wavelength of $\lambda = 1064$ nm was used as the incident light.

Glass fibers with a diameter of $\sim 100\,\mu m$ were prepared by pulling up the melt using a silica glass rod, where the pulling rate of the silica rod is ~ 1 m/s. In this method, the fibers were prepared by a hand-operated technique, but not using any fiber drawing machine. Then, the glass fibers were heat treated to obtain transparent nanocrystallized glass fibers. Glass and nanocrystallized fibers were etched using a meniscus chemical etching method [24], in which etching solutions such as 10 M-NaOH/hexane and 10 wt%-HF/hexane were used.

3. Results and discussion

3.1. Characterization of $KNb(Ge,Si)O_5$ glasses

The glasses with the chemical compositions of $25K_2O$–$25Nb_2O_5$–$50GeO_2$, $25K_2O$–$25Nb_2O_5$–$25GeO_2$–$25SiO_2$ and $25K_2O$–$25Nb_2O_5$–$50SiO_2$ were prepared in this study, and they are designated here as KNG, KNGS, and KNS, respectively. The DTA patterns for bulk KNG, KNGS and KNS glasses are shown in Fig. 1. All these glasses show clear endothermic peaks due to the glass transition and exothermic peaks due to the crystallization. The values of T_g and T_p are summarized in Table 1. It is seen that the glass transition and crystallization peak temperatures increase when the amount of SiO_2 increases. Furthermore, it is noted that KNG glass shows one sharp crystallization peak, but two peaks are observed in KNS glass. KNGS glass has one crystallization peak, but its shape is broad. These results indicate that KNG and KNS glasses show different crystallization behaviors.

Table 1
Glass compositions, values of glass transition T_g, crystallization peak T_p temperatures, density d, and refractive index n in K_2O–Nb_2O_5–GeO_2–SiO_2 glasses examined in the present study

Sample	Composition (mol%)				T_g (°C)	T_p (°C)	d (g/cm^3)	n
	K_2O	Nb_2O_5	GeO_2	SiO_2	(±3 °C)	(±3 °C)	(±0.01)	(±0.01)
KNG	25	25	50	—	619	679	3.83	1.81
KNGS	25	25	25	25	655	720	3.60	1.77
KNS	25	25	—	50	670	761	3.34	1.75

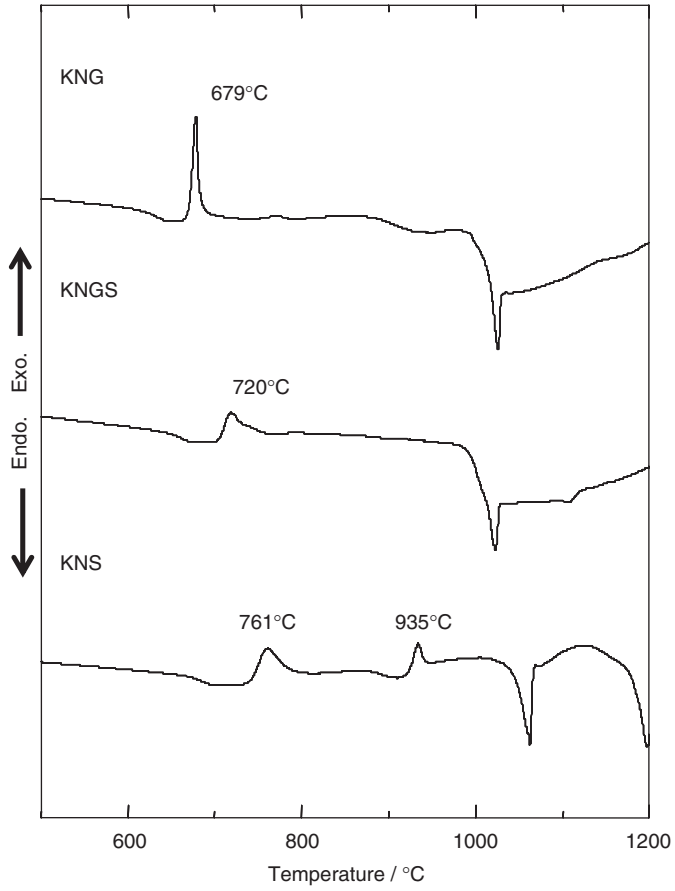

Fig. 1. DTA patterns for bulk $25K_2O$–$25Nb_2O_5$–$(50-x)GeO_2$–$xSiO_2$ glasses. Heating rate was 10 K/min. KNG for $x = 0$, KNGS for $x = 25$, and KNS for $x = 50$.

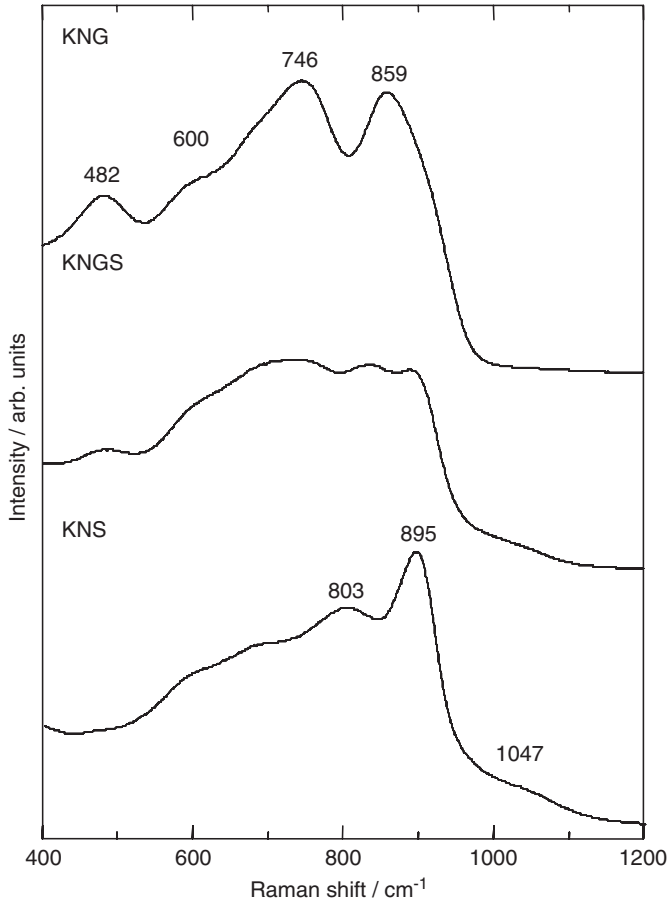

Fig. 2. Raman scattering spectra at room temperature for $25K_2O$–$25Nb_2O_5$–$(50-x)GeO_2$–$xSiO_2$ glasses. KNG for $x = 0$, KNGS for $x = 25$, and KNS for $x = 50$.

The values of d and n are also given in Table 1. It is clear that both values increase when the amount of GeO_2 increases. Since the optical basicity ($\Lambda = 0.70$ or 0.63), i.e., electron donor ability, of GeO_2 oxide is larger than that ($\Lambda = 0.48$) of SiO_2 oxide [25–27], it is expected that KNG glass would give a large refractive index compared with KNS glass, as observed in this study. The optical basicity ($\Lambda = 1.05$) of Nb_2O_5 oxide is large [25], and thus all KNG, KNGS and KNS glasses with 25 mol% Nb_2O_5 indicate relatively large refractive indices of $n = 1.75-1.81$.

The Raman scattering spectra at room temperature for KNG, KNGS, and KNS glasses are shown in Fig. 2. It is well known that structural units of NbO_6 octahedra, GeO_4 and SiO_4 tetrahedra in glasses give clear peaks in Raman scattering spectra, and, therefore, it would be worth summarizing features of Raman spectra of glasses containing Nb_2O_5, GeO_2 and SiO_2 reported in many papers. According to Fukumi and Sakka [28,29], the Raman band in the 800–900 cm^{-1} region in glasses such as K_2O–Nb_2O_5–SiO_2 is attributed to NbO_6 octahedra with non-bridging oxygens and/or with much distortions and the broad bands in the 600–800 cm^{-1} region are attributed to less-distorted NbO_6 octahedra with no non-bridging oxygens. For GeO_2- and SiO_2-based glasses, Raman scattering spectra (i.e., peak position and intensity) relating to vibrations of GeO_4 and SiO_4 tetrahedra change significantly depending on the type and amount of network modifier cations. Basically, however, for GeO_2-based glasses, bands in the mid-frequency region of ~400–~500 cm^{-1} are assigned to stretching vibrations of Ge–O–Ge bonds (bridge) associated with four- and three-membered GeO_4 rings, and bands in the high-frequency region of ~850 cm^{-1} are assigned to stretching vibrations of Ge–O^- bonds (terminal groups) [30–32]. In Raman scattering spectra for SiO_2-based glasses, analyzes similar to GeO_2-based glasses have been performed. That is, bands ~1100 cm^{-1} are assigned to stretching vibrations of Si–O^- bonds (SiO_4 terminal groups with non-bridging oxygens) and bands in the 400–700 cm^{-1} region are assigned to bending vibrations of Si–O–Si linkages between SiO_4 teterahera [33–35]. As the polarizability of Nb–O bonds is higher than that of Si–O bonds, generally the most intensive bands in Raman scattering spectra for SiO_2-based glasses with large amounts of Nb_2O_5 are related to vibrational modes of NbO_6 octahedra [15].

As can be seen in Fig. 2, peaks are observed at ~480 cm^{-1} for KNG and KNGS glasses containing GeO_2, but not in KNS glass. This peak would be,

therefore, assigned to stretching vibrations of Ge–O–Ge bonds between GeO_4 teterahera. In KNG glass, a strong peak is observed at 859 cm^{-1}, and this peak would indicate the presence of GeO_4 tetrahedra with non-bridging oxygens. In KNGS and KNS glasses containing SiO_2, peaks are observed at ~1050 cm^{-1}, although their peak intensities are small. These peaks would be assigned to stretching vibrations of $Si–O^-$ bonds. The Raman scattering spectra, therefore, indicate that GeO_4 and SiO_4 tetrahedra are clearly formed in $K_2O–Nb_2O_5–GeO_2$ or SiO_2 glasses with large amounts (50 mol%) of K_2O and Nb_2O_5. The peaks with similar intensities are observed at ~600 cm^{-1} for KNG, KNGS and KNS glasses, suggesting the presence of less-distorted NbO_6 octahedra with no non-bridging oxygens. Furthermore, a strong shoulder for KNG glass and strong peaks for KNGS and KNS glasses are observed at 900 cm^{-1}. Since no bands have been usually observed at ~900 cm^{-1} in silicate glasses, it would be reasonable to assign that these peaks at ~900 cm^{-1} are due to NbO_6 octahedra, i.e., NbO_6 octahedra with non-bridging oxygens and/or with much distortions.

Kolobkova [36] reported the Raman scattering spectrum for $25K_2O–25Nb_2O_5–50GeO_2$ glass and proposed the peak assignments similar to the present study. The Raman scattering spectrum for $23K_2O–27Nb_2O_5–50SiO_2$ glass has been reported by Aronne et al.[15], and they concluded that the structure of the glass is formed by SiO_4 tetrahedra and distorted NbO_6 octahedra. In particular, they assigned that the Raman band at 900 cm^{-1} is related to the vibration of highly distorted octahedral NbO_6 or to ocathedral NbO_6 having at least a short terminal Nb–O bond pointing towards a modifier ion. Contrary, Alekseeva et al.[14] proposed that the Raman band at 895 cm^{-1} observed for $25K_2O–27.5Nb_2O_5–47.5SiO_2$ glass corresponds to the vibrations of NbO_4 tetrahedra and other two bands at ~780 and ~690 cm^{-1} are associated with the vibrations of the slightly distorted NbO_6 octahedra with no non-bridging oxygen atoms. Although the Raman scattering spectra for $25K_2O–25Nb_2O_5–50SiO_2$ (present study), $23K_2O–27Nb_2O_5–50SiO_2$ [15], and $25K_2O–27.5Nb_2O_5–47.5SiO_2$ [14] glasses have almost the same patterns, the interpretation of the band at ~900 cm^{-1} is still open to discussion. Considering the Raman scattering spectra for various niobium oxides with NbO_6 and NbO_4 coordinated units [37], however, it seems to be reasonable to assign that the peak at 895 cm^{-1} observed for $25K_2O–25Nb_2O_5–50SiO_2$ glass (Fig. 2) is related to distorted NbO_6 octahedra, as proposed by Fukumi and Sakka [28,29] and Aronne et al.[15].

3.2. Formation of nanocrystals in $KNb(Ge,Si)O_5$ glasses

KNG, KNGS, and KNS glasses were heat treated at their first crystallization peak temperatures for 1 h, and the results on the XRD analyzes for the powder (pulverized) samples are shown in Fig. 3. The broad peaks suggest the formation of nanoscaled crystals in these heat-treated samples. The optical transmittance spectra for these crystallized glasses are shown in Fig. 4, indicating that the absorption edge is around 330 nm and the transmittance in the visible wavelength region is around 70%. As already clarified in previous studies [7–9], KNG glass shows a prominent bulk nanocrystallization, in which the crystalline phase is $K_{3.8}Nb_5Ge_3O_{20.4}$ ([38] and JCPDS 77-0963) and the size of nanocrystals is 10–30 nm. As an example, a transmittance electron microscope (TEM: JEM-3000F operating at 300 kV) image for the heat-treated (720 °C, 1 h) KNG sample is shown in Fig. 5. It is clearly confirmed the formation of nanocrystals with a diameter of ~20 nm. In the previous papers [7,8], it has been proposed from the density measurements that the volume fraction of $K_{3.8}Nb_5Ge_3O_{20.4}$ nanocrystals formed in the bulk KNG crystallized (680 °C, 1 h) glass is about 60%. The results shown in Figs. 3–5 indicate that the nanocrystallization occurs not only in $25K_2O–25Nb_2O_5–50GeO_2$ glass but also in $25K_2O–25Nb_2O_5–25GeO_2–25SiO_2$ and $25K_2O–25Nb_2O_5–50SiO_2$ glasses. Certainly, the formation of nanocrystals has been proposed in $K_2O–Nb_2O_5–SiO_2$ glasses, although the structure and chemical composition of nanocrystals have not been clarified [10–15].

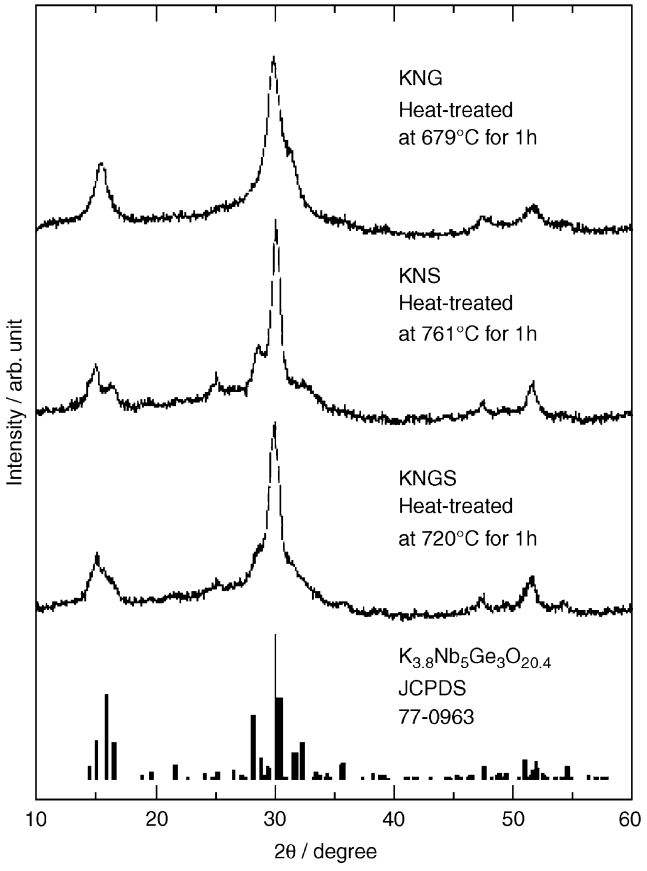

Fig. 3. Powder XRD patterns at room temperature for the crystallized glasses obtained by heat treatments at the crystallization peak temperatures for 1 h in the $25K_2O–25Nb_2O_5–(50–x)GeO_2–xSiO_2$ system. KNG for $x = 0$, KNGS for $x = 25$, and KNS for $x = 50$.

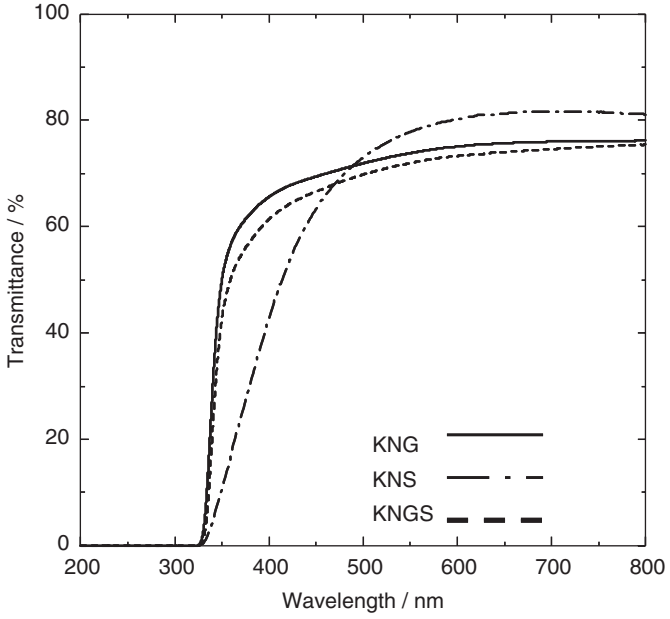

Fig. 4. Optical transmission spectra for the crystallized samples in the $25K_2O$–$25Nb_2O_5$–$(50-x)GeO_2$–$xSiO_2$ system. The heat-treatment temperatures are 679 °C for KNG ($x = 0$), 720 °C for KNGS ($x = 25$), and 761 °C for KNS ($x = 50$). The heat-treatment time was 1 h for all samples.

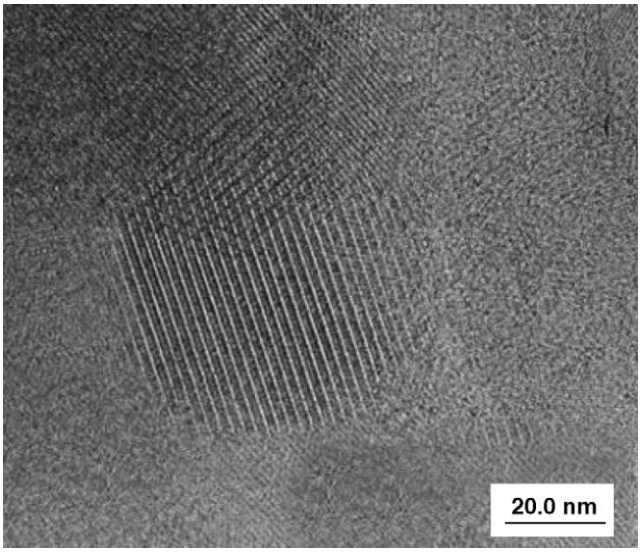

Fig. 5. TEM image for the crystallized (720 °C, 1 h) glass of $25K_2O$–$25Nb_2O_5$–$50GeO_2$.

According to Belokoneva et al.[38], the $K_{3.8}Nb_5Ge_3O_{20.4}$ phase, which is prepared by cooling slowly (2 K/h) the melt of $25K_2O$–$25Nb_2O_5$–$50GeO_2$ in the temperature range of 1100–700 °C, has an orthorhombic structure with the lattice constants of $a = 0.7064$, $b = 1.2177$, and $c = 2.2113$ nm. It is known that the structure of the $K_{3.8}Nb_5Ge_3O_{20.4}$ phase consists of three-membered tetrahedral rings formed by GeO_4 tetrahedra, NbO_6 octahedra linked to Ge_3O_9 rings, and NbO_6 octahedra connected to other NbO_6 octahedra [38]. It should be pointed out that GeO_4 tetrahedra are somewhat distorted and five different NbO_6 octahedra are present [38].

As can be seen in Fig. 3, the XRD patterns for KNGS and KNS glasses are similar to KNG glass, suggesting that nanocrystals similar to $K_{3.8}Nb_5Ge_3O_{20.4}$, i.e., $K_{3.8}Nb_5(Ge,Si)_3O_{20.4}$ and $K_{3.8}Nb_5Si_3O_{20.4}$, might be formed due to the crystallization at T_p. The crystallization behavior of K_2O–Nb_2O_5–SiO_2 glasses has been examined some research groups [10–15], and it has been reported that unidentified (metastable) crystalline phases are formed due to the crystallization besides the stable phases of $K_3Nb_3Si_2O_{13}$, $KNbSi_2O_7$ and $KNbO_3$. The present study suggests that one of the metastable crystalline phases formed in K_2O–Nb_2O_5–GeO_2–SiO_2 crystallized glasses is close to $K_{3.8}Nb_5(Ge,Si)_3O_{20.4}$.

The Raman scattering spectra for KNG, KNGS, and KNS crystallized glasses obtained by heat treatments at T_p for 1 h are shown in Fig. 6. It is seen that these spectra are considerably different from those (Fig. 2) for the precursor glasses. As a trend, the relative intensity of the bands observed at above 700 cm^{-1} against the bands observed at below 700 cm^{-1} is becoming small due to the nanocrystallization. Furthermore, it should be pointed out that nanocrystals formed in these heat-treated samples give

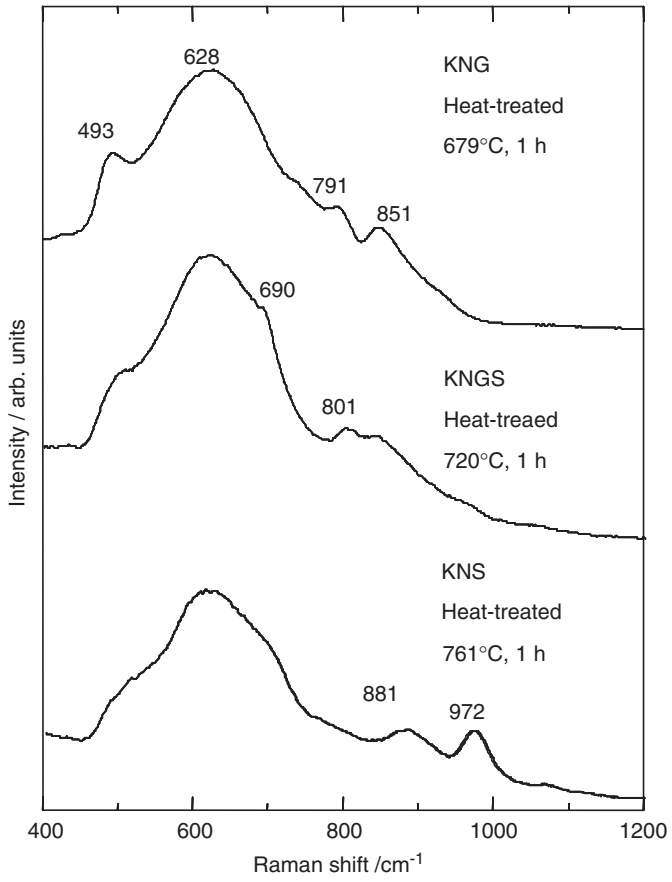

Fig. 6. Raman scattering spectra at room temperature for the crystallized glasses obtained by heat treatments at the crystallization peak temperatures for 1 h in the $25K_2O$–$25Nb_2O_5$–$(50-x)GeO_2$–$xSiO_2$ system. KNG for $x = 0$, KNGS for $x = 25$, and KNS for $x = 50$.

extremely broad Raman bands. In all samples, broad and strong bands are observed at around 600 cm^{-1}. Considering the structure of $K_{3.8}Nb_5Ge_3O_{20.4}$ crystals, the main contribution to the bands at ~600 cm^{-1} would be due to the five different NbO_6 octahedra. That is, it is considered that the amount of distorted NbO_6 octahedra giving the Raman bands at around 900 cm^{-1} observed in the precursor glasses (Fig. 2) decreases due to the nanocrystallization. The Raman spectra for the heat-treated sample of $25K_2O$–$25Nb_2O_5$–$50SiO_2$ glass (Fig. 6) are almost the same as those for $23K_2O$–$27Nb_2O_5$–$50SiO_2$ [15], and $25K_2O$–$27.5Nb_2O_5$–$47.5SiO_2$ [14] glasses. The SH intensity for these transparent crystallized (heat-treated at T_p for 1 h) glasses consisting of nanocrystals were examined, but no measurable SHGs were detected. It is, therefore, concluded that the $K_{3.8}Nb_5Ge_3O_{20.4}$ crystalline phase has an inversion symmetry in the structure, i.e., isotropic, and the substitution of Ge^{4+} for Si^{4+} do not break the inversion symmetry in the $K_{3.8}Nb_5Ge_3O_{20.4}$ phase.

The powder XRD patterns for the crystallized glasses obtained by heat treatments at temperatures (850, 900, 935 °C) higher than T_p are shown in Fig. 7. In KNG sample, the crystalline phase of $K_{3.8}Nb_5Ge_3O_{20.4}$ is still present, and a relatively good transparency is still seen, as already reported in the previous papers [7,8]. But, in KNGS and KNS samples, the crystalline phase is not $K_{3.8}Nb_5(Ge,Si)_3O_{20.4}$, and a transparency is disappeared.

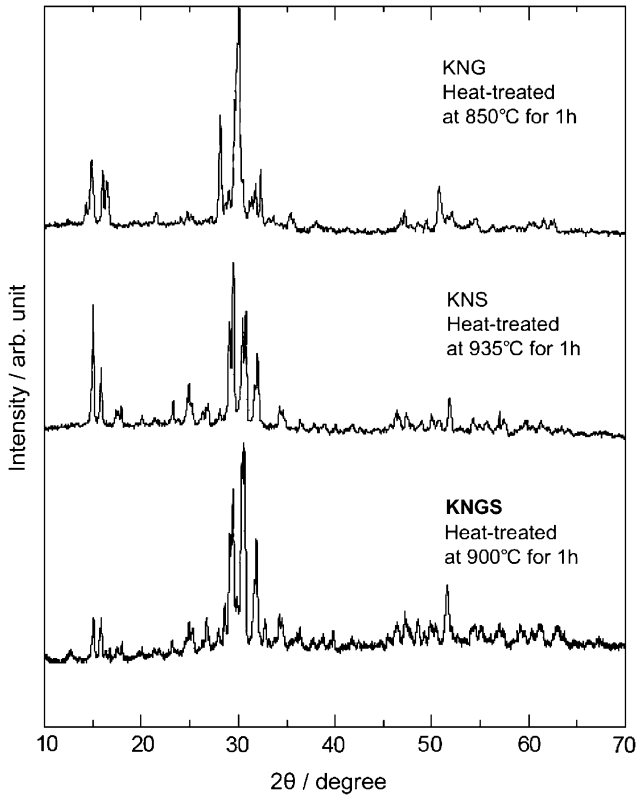

Fig. 7. Powder XRD patterns at room temperature for the crystallized glasses in the $25K_2O$–$25Nb_2O_5$–$(50-x)GeO_2$–$xSiO_2$ system. KNG for $x = 0$, KNGS for $x = 25$, and KNS for $x = 50$.

Unfortunately, the crystalline phases in these crystallized samples have not been identified at this moment, but the crystalline phases close to $K_{3.8}Nb_5(Ge,Si)_3O_{20.4}$, i.e., the modified structure, are considered to be formed because of similar XRD patterns for these three samples as shown in Fig. 7. Since the transparency was disappeared for these crystallized KNGS and KNS glasses and the XRD peaks are relatively sharp, it is concluded that the growth of nanocrystals occurs in these KNGS and KNS samples. That is, it is considered that SiO_2-substututed $K_{3.8}Nb_5(Ge,Si)_3O_{20.4}$ nanocrystals might be unstable thermally in comparison with $K_{3.8}Nb_5Ge_3O_{20.4}$ nanocrystals.

From the above experiments, we clarified that all KNG, KNGS, and KNS glasses show nanocrystallization and transparent nanocrystallized glasses can be obtained through the crystallization at around the first crystallization peak temperatures. In particular, it was found that the nanocrystallization behavior of K_2O–Nb_2O_5–GeO_2–SiO_2 glasses depends on the GeO_2/SiO_2 ratio. These transparent nanocrystallized glasses do not show, however, any SHGs even for the substitution of GeO_2 for SiO_2.

The dielectric constants (frequency: 1 kHz, temperature: room temperature, apparatus: TOYO corp. FCE-1 model), ε, of the glasses and nanocrystallized glasses obtained by heat treatments at the first crystallization peak temperature for 1 h were measured, and the following values were obtained: $\varepsilon = 43, 41,$ and40 for KNG, KNGS, and KNS glasses, respectively, and $\varepsilon = 58, 59,$ and49 for KNG, KNGS, and KNS nanocrystallized glasses, respectively. These results clearly indicate that the dielectric constant of K_2O–Nb_2O_5–GeO_2–SiO_2 glasses increases largely due to the nanocrystallization.

3.3. Chemical etching of nanocrystallized $KNbGeO_5$ glass fibers

KNG glass fibers with a diameter of ~100 μm were prepared by inserting a silica glass rod into a melt and by pulling up the rod from the melt. The glass fibers obtained were heat treated at 680 °C for 1 h. It was found that transparent nanocrystallized glass fibers are successfully fabricated as similar to the case of bulk plate glasses. Considering the volume fraction of $K_{3.8}Nb_5Ge_3O_{20.4}$ nanocrystals formed in the bulk (not fibers) KNG crystallized (680 °C, 1 h) glass [7,8], i.e., 60%, it would be expected that the crystallized glass fibers also have a similar volume fraction (60%) of $K_{3.8}Nb_5Ge_3O_{20.4}$ nanocrystals. The base glass fibers and nanocrystallized glass fibers were etched using a meniscus chemical etching method [18,20,21,24], in which the etching solutions of 10 wt%-HF/hexane and 10 M-NaOH/hexane were used. In this etching technique, it is expected that the evolution of a meniscus at the interface between the fiber and the solution leads to the tip formation, and hexane is used as a protecting overlayer against HF or NaOH etching solution. It is well recognized that network structures such as Si–O–Si bonds in oxide glasses are attacked and broken by acid solutions such as

F^- ions in HF or alkali solutions such as OH^- ions in NaOH. There has been no report on chemical etching behaviors in GeO_2-based glasses and crystallized glasses, and thus we tried to use both aqueous HF and NaOH solutions in this study.

The polarization optical microphotographs for the KNG glass fiber etched chemically using the 10 wt%-HF/hexane system are shown in Fig. 8. The temperature of the etching solution was fixed to room temperature, and the etching time was 2 h. It is seen that the taper length is about 270 μm and the tip angle is about 23°. Although the tip (aperture size) is not a nanoscaled size, the data shown in Fig. 8 demonstrate that the 10 wt%-HF/hexane system works as an etching solution for KNG glass fibers. The polarization optical microphotographs for the transparent KNG nanocrystallized glass fiber etched chemically using the 10 wt%-HF/hexane system are shown in Fig. 9. It is clear that the etched shape is different from that for the precursor glass fiber (Fig. 8). That is, the taper length is about 450 μm and the tip angle is about 12°. These results indicate that the meniscus state and etching rate for the nanocrystallized KNG glass fibers in the 10 wt%-HF/hexane system is different from those for the precursor KNG glass fibers. In other words, it is considered that nanocrystals themselves and grain boundaries among nanocrystals in nanocrystallized glass fibers affects largely the etching behavior.

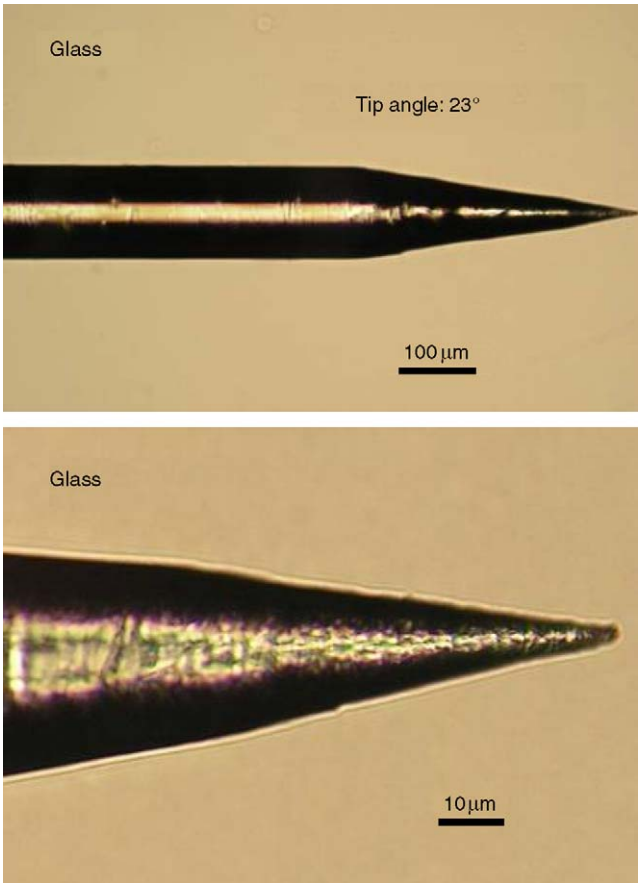

Fig. 8. Polarization optical microphotographs for the glass fiber etched (room temperature, 2 h) chemically using the 10 wt%-HF/hexane system. The glass composition is $25K_2O$–$25Nb_2O_5$–$50GeO_2$.

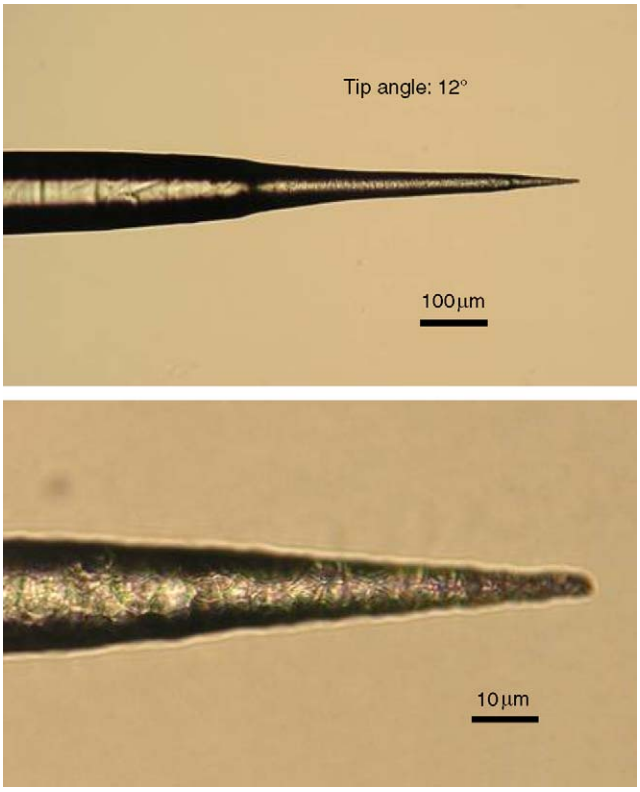

Fig. 9. Polarization optical microphotographs for the nanocrystallized glass fiber etched (room temperature, 2 h) chemically using the 10 wt%-HF/hexane system. The glass composition is $25K_2O$–$25Nb_2O_5$–$50GeO_2$.

The polarization optical microphotographs for the transparent KNG nanocrystallized glass fiber etched chemically (at room temperature for 2 weeks) using the 10 M-NaOH/hexane system are shown in Fig. 10. It was found that the etching rate is very low, and a long etching time, i.e., 2 weeks, was needed to get sharpened fibers. As shown in Fig. 10, the taper length is about 2 mm, the tip angle is about 3°, and the shape of fiber tip is not sharp. These results indicate that the 10 M-NaOH/hexane system is not so effective for the etching of KNG nanocrystallized glass fibers compared with the 10 wt%-HF/hexane system.

It is known that the optical resolution in SNOM is of the order of the size of the probe aperture [39,40], and thus it is important to fabricate optical fiber probes with a nanoscaled aperture. It is desired to examine the etching behavior of transparent nanocrystallized glass fibers in various etching solutions and to find optimal etching solutions and conditions for the fabrication of fiber probes with a nanoscaled aperture. The transparent $KNb(Ge,Si)O_5$ nanocrystallized glasses have the refractive indices of $n = 1.75-1.81$ and the dielectric constants of $\varepsilon = 50-59$, being much higher than those ($n = 1.45$, $\varepsilon = 4$) for SiO_2 glass. This would be a strong motivation for the study of nanocrystallized glass fiber probes in the K_2O–Nb_2O_5–GeO_2–SiO_2 glass system.

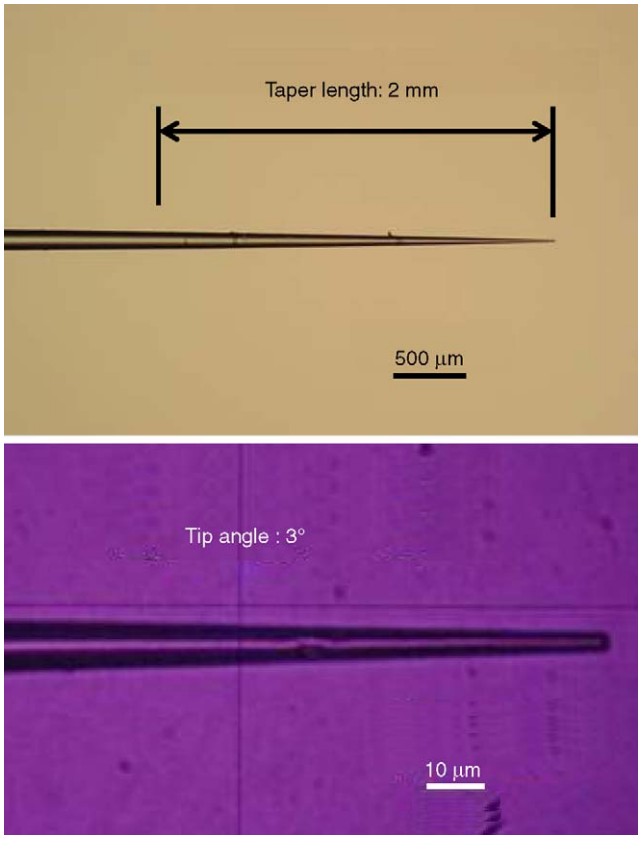

Fig. 10. Polarization optical microphotographs for the nanocrystallized glass fiber etched (room temperature, 2 weeks) chemically using the 10 M-NaOH/hexane system. The glass composition is $25K_2O$–$25Nb_2O_5$–$50GeO_2$.

The mechanical properties such as Young's modulus and Vickers hardness of transparent KNG nanocrystallized glass fibers fabricated in this study have not been clarified at this moment. In the previous papers [7,8], the author group clarified that the elastic and mechanical properties of bulk KNG glass are largely improved due to the nanocrystallization. For instance, KNG glass has the values of Young's modulus $E = 64$ GPa and Debye temperature $\theta_D = 500$ K, but the transparent nanocrystallized (heat-treated at 630 °C, 1 h) glass shows $E = 81$ GPa and $\theta_D = 564$ K. It is expected that transparent KNG nanocrystallized glass fibers would have elastic and mechanical properties similar to bulk transparent KNG nanocrystallized bulk glasses.

4. Conclusion

The crystallization behavior of $25K_2O$–$25Nb_2O_5$–$(50-x)GeO_2$–$xSiO_2$ glasses with $x = 0$, 25, and 50 (i.e., $KNb(Ge,Si)O_5$ glasses) was examined to fabricate transparent nanocrystallized glasses showing SHGs. In all compositions, transparent nanocrystallized glasses were obtained through the crystallization at first crystallization peak temperatures, although they did not show measurable SHGs. The glass fibers with a diameter of about 100 μm were fabricated by just pulling up the melt using a silica rod, and transparent nanocrystallized glass fibers were produced by heat treatments of the precursor glass fibers. The fibers with sharpened tips (e.g., the taper length is about 450 μm and the tip angle is about 12°) were obtained using a meniscus chemical etching method, in which the etching solutions of 10 wt%-HF/hexane and 10 M-NaOH/hexane were used.

Acknowledgments

This work was supported from the Grant-in-Aid for Scientific Research from the Ministry of Education, Science, Sport, and Culture, Japan, and by the 21st Century Center of Excellence (COE) Program in Nagaoka University of Technology. The authors also would like to thank Hosokawa Powder Technology Foundation for the partial financial support to this work.

References

[1] G.H. Beall, D.A. Duke, J. Mater. Sci. 4 (1969) 340.
[2] K. Shioya, T. Komatsu, H.G. Kim, K. Matusita, J. Non-Cryst. Solids 189 (1995) 16.
[3] R. Sakai, Y. Benino, T. Komatsu, Appl. Phys. Lett. 77 (2000) 2118.
[4] N. Tamagawa, Y. Benino, T. Fujiwara, T. Komatsu, Opt. Commun. 217 (2003) 387.
[5] K. Naito, Y. Benino, T. Fujiwara, T. Komatsu, Solid State Commun. 131 (2004) 289.
[6] Y. Takahashi, K. Kitamura, Y. Benino, T. Fujiwara, T. Komatsu, Appl. Phys. Lett. 86 (2005) 091110.
[7] F. Torres, K. Narita, Y. Benino, T. Fujiwara, T. Komatsu, J. Appl. Phys. 94 (2003) 5265.
[8] K. Narita, Y. Takahashi, Y. Benino, T. Fujiwara, T. Komatsu, T. Hanada, Y. Hirotsu, J. Am. Ceram. Soc. 87 (2004) 113.
[9] K. Narita, Y. Takahashi, Y. Benino, T. Fujiwara, T. Komatsu, Opt. Mater. 25 (2004) 393.
[10] V.N. Sigaev, S.Yu. Stefanovich, B. Champagnon, I. Gregora, P. Pernice, A. Aronne, R. LeParc, P.D. Sarkisov, C. Dewhurst, J. Non-Cryst. Solids 306 (2002) 238.
[11] H. Tanaka, M. Yamamoto, Y. Takahashi, Y. Benino, T. Fujiwara, T. Komatsu, Opt. Mater. 22 (2003) 71.
[12] V.N. Sigaev, S.Yu. Stefanovich, B. Champagnon, I. Gregora, P. Pernice, A. Aronne, R. LeParc, P.D. Sarkisov, C. Dewhurst, J. Non-Cryst. Solids 306 (2002) 238.
[13] A. Aronne, V.N. Sigaev, P. Pernice, E. Fanelli, L.Z. Usmanova, J. Non-Cryst. Solids 337 (2004) 121.
[14] I.P. Alekseeva, V.V. Golubkov, O.S. Dymshits, A.A. Zhilin, V.I. Petrov, M.Ya. Tsenter, Glass Phys. Chem. 30 (2004) 311.
[15] A. Aronne, V.N. Sigaev, B. Champagnon, E. Fanelli, V. Califano, L.z. Usmanova, P. Pernice, J. Non-Cryst. Solids 351 (2005) 3610.
[16] P.A. Tick, N.F. Borrelli, I.M. Reaney, Opt. Mater. 15 (2000) 81.
[17] B.N. Samson, P.A. Tick, N.F. Borrelli, Opt. Lett. 26 (2001) 145.
[18] N. Iwafuchi, S. Mizuno, Y. Benino, T. Fujiwara, T. Komatsu, M. Koike, K. Matusita, Adv. Mater. Res., in press.
[19] S. Monomobe, M. Naya, T. Saiki, M. Ohtsu, Appl. Opt. 36 (1997) 1496.
[20] A. Sayah, C. Philipona, P. Lambelet, M. Pfeffer, F. Marquis-Weible, Ultramicroscopy 71 (1998) 59.
[21] R. Micheletto, N. Yoshimatsu, S. Okazaki, Opt. Commun. 188 (2001) 11.
[22] M. Ohtsu, K. Kobayashi, Basis of Near-Field Light, Ohmsha, Tokyo, 2003, p. 74, 93 (in Japanese).
[23] S.K. Kurtz, T.T. Perry, J. Appl. Phys. 39 (1968) 3798.

[24] D.R. Turner, Etch procedure for optical fibers, US Patent, 4469, 554, 1983.
[25] V. Dimitrov, S. Sakka, J. Appl. Phys. 79 (1996) 1736.
[26] V. Dimitrov, T. Komatsu, J. Solid State Chem. 178 (2005) 831.
[27] E.I. Kamitsos, Y.D. Yiannopoulos, J.A. Duffy, J. Phys. Chem. B 106 (2002) 8988.
[28] K. Fukumi, S. Sakka, J. Mater. Sci. 23 (1988) 2819.
[29] K. Fukumi, S. Sakka, J. Non-Cryst. Solids 110 (1989) 61.
[30] D.A. McKeown, C.I. Mertzbacher, J. Non-Cryst. Solids 183 (1995) 61.
[31] A.M. Efimov, J. Non-Cryst. Solids 253 (1999) 95.
[32] G.S. Henderson, R.T. Amos, J. Non-Cryst. Solids 328 (2003) 1.
[33] D.W. Matson, S.K. Sharma, J.A. Philpotts, J. Non-Cryst. Solids 58 (1983) 323.
[34] P. McMillan, Am. Mineral. 69 (1984) 622.
[35] J.R. Allwardt, B.C. Schmidt, J.F. Stebbins, Chem. Geol. 213 (2004) 137.
[36] E.V. Kolobkova, Fiz. Khim. Stekla 13 (1987) 352.
[37] J.M. Jehng, I.E. Wachs, Chem. Mater. 3 (1991) 100.
[38] E.L. Belokoneva, B.V. Mill, A.V. Butashin, Russ. Inorg. Chem. 38 (1993) 1356.
[39] E. Betzig, J.T. Trautman, Science 257 (1992) 189.
[40] L. Novotny, D.W. Pohl, B. Hecht, Opt. Lett. 20 (1995) 970.